Electron Transfer Photochemistry of a Bridged Norcaradiene: A Mechanistic Probe for Radical Cation Nucleophilic Capture

Torsten Herbertz, Florian Blume, and Heinz D. Roth*

Contribution from the Department of Chemistry, Wright-Rieman Laboratories, Rutgers University, New Brunswick, New Jersey 08854-8087

Received September 11, 1997

Abstract: The radical cation of tricyclo[4.3.1.0^{1,6}]deca-2,4-diene (**3**) can be generated by electron transfer to 1,4-dicyanobenzene (DCB) in acetonitrile/methanol; the species is captured by regiospecific nucleophilic attack of methanol in the 2- (and 5-) position. On the other hand, the reaction shows little stereochemical preference. The resulting allylic radical reacts by aromatic substitution on the radical anion of DCB, the 3-position serving as the principal site of coupling. Remarkably, the cyclopropane function of **3**$^{\bullet+}$ is not a target of nucleophilic attack, even though the secondary cyclopropane carbon has spin and charge density. The observed reaction is compatible with a theoretical model proposed by Shaik and Pross, which correlates radical cation reactivity with the spin density of the corresponding triplet state. The capture of **3**$^{\bullet+}$ occurs in the position where both SOMO and LUMO have significant orbital coefficients.

Introduction

The structures and reactions of organic radical cations have attracted much attention during the past two decades.[1,2] Especially, molecules containing strained ring moieties as well as unsaturated functions have been studied in considerable detail. We are interested in conjugative and homoconjugative interactions in substrates containing olefinic moieties and cyclopropane rings. We have evaluated how these interactions affect the structures of the resulting radical cations, particularly the distribution of spin and charge.[2e,3] We have also probed whether homoconjugation manifests itself in the reactivities of the radical cations, particularly in the regiochemistry of nucleophilic capture. For example, we have derived the hyperfine coupling patterns of radical cations from CIDNP results and compared them with the reactivity patterns derived from the products obtained in photoinduced electron-transfer reactions. Thus, the radical cations of 7-methylenenorbornadiene (**MN**) and 7-methylenequadricyclane (**MQ**) react at the pairs of olefinic or cyclopropane moieties, but fail to undergo nucleophilic capture at the exocyclic double bonds,[4] despite significant spin density in the exo-methylene bond of **MN**$^{\bullet+}$ as indicated by CIDNP results.[5] The high degree of regio- (and stereo-) selectivity observed for **MN**$^{\bullet+}$ led to the current study of the norcaradiene system, **1**, in which we evaluate the homoconjugation between the butadiene and cyclopropane moieties.

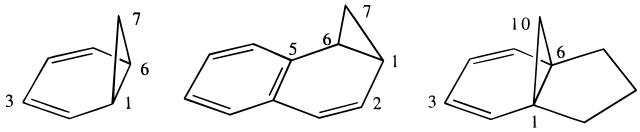

1 **2** **3**

Earlier, we assigned a unique structure to the radical cation of benzonorcaradiene (**2**), with spin density on the secondary cyclopropane carbon.[6] The radical cations of **1** and of the bridged derivative tricyclo[4.3.1.0^{1,6}]deca-2,4-diene (**3**)[7] are expected to have a similar structure; thus, the spin density at C_{10} may direct nucleophilic capture to this carbon. This attack is energetically favorable, as it relieves the strain of the cyclopropane ring and forms a highly delocalized free radical. We have applied a 2-fold approach to evaluate the extent of homoconjugation in radical cations of norcaradiene systems. We studied the electron-transfer photochemistry of the bridged derivative **3** in the presence of methanol as a nucleophile and carried out *ab initio* calculations on the radical cations of **1**−**3**. This study identifies **3** as a unique probe elucidating mechanistic features of the nucleophilic capture of radical cations.

The radical cation, **3**$^{\bullet+}$, is generated by an indirect pathway, involving the following steps: irradiation of a cosensitizer (phenanthrene, **Ph**) with light of $\lambda \geq 350$ nm (eq 1); electron transfer from ^{1}**Ph*** to 1,4-dicyanobenzene (**DCB**), generating the radical ion pair, **Ph**$^{\bullet+}$−**DCB**$^{\bullet-}$ (eq 2); and a secondary

(1) (a) Forrester, R. A.; Ishizu, K.; Kothe, G.; Nelsen, S. F.; Ohya-Nishiguchi, H.; Watanabe, K.; Wilker, W. Organic Cation Radicals and Polyradicals. In *Landolt Börnstein, Numerical Data and Functional Relationships in Science and Technology*; Springer-Verlag: Heidelberg, 1980; Vol. IX, Part d2. (b) Yoshida, K. *Electrooxidation in Organic Chemistry: The Role of Cation Radicals as Synthetic Intermediates*; Wiley: New York, 1984. (c) Shida, T. *Electronic Absorption Spectra of Radical Ions*; Elsevier: Amsterdam, 1988. (d) *Radical Ionic Systems*; Lund, A., Shiotani, M., Eds.; Kluwer Academics: Dordrecht, 1991.

(2) (a) Ledwith, A. *Acc. Chem. Res.* **1972**, *5*, 133−139. (b) Shida, T.; Haselbach, E.; Bally, T. *Acc. Chem. Res.* **1984**, *17*, 180−186. (c) Nelsen, S. F. *Acc. Chem. Res.* **1987**, *20*, 269−215. (d) Bauld, N.; Bellville, D. J.; Harirchian, B.; Lorenz, K. T.; Pabon, R. A., Jr.; Reynolds, D. W.; Wirth, D. D.; Chiou, H.-S.; Marsh, B. K. *Acc. Chem. Res.* **1987**, *20*, 180−186. (e) Roth, H. D. *Acc. Chem. Res*. **1987**, *20*, 343−370. (f) Mirafzal, G. A.; Liu, J.; Bauld, N. *J. Am. Chem. Soc.* **1993**, *115*, 6072.

(3) Roth, H. D. *Top. Curr. Chem.* **1992**, *163*, 131−245.

(4) Weng, H.; Du, X.; Roth, H. D. *J. Am. Chem. Soc.* **1995**, *117*, 135−140.

(5) Roth, H. D.; Du, X.-M.; Weng, H.; Lakkaraju, P. S.; Abelt, C. J. *J. Am. Chem. Soc.* **1994**, *116*, 7744−7752.

(6) (a) Roth, H. D.; Schilling, M. L. M. *Can. J. Chem.* **1983**, *61*, 1027. (b) Roth, H. D.; Schilling, M. L. M.; Schilling, F. C. *J. Am. Chem. Soc.* **1985**, *107*, 4152.

(7) Vogel, E.; Wiedemann, W.; Roth, H. D.; Eimer, J.; Günther, H. *Liebigs Ann. Chem.* **1972**, *759*, 1−36.

S0002-7863(97)03203-4 CCC: $15.00
Published on Web 05/05/1998

electron transfer from **3** to $\mathbf{Ph}^{\bullet+}$ generating a secondary radical ion pair, $\mathbf{3}^{\bullet+}-\mathbf{DCB}^{\bullet-}$ (eq 3). When generated in the presence of a nucleophile (5 M CH_3OH), this pair undergoes a well-established photochemical reaction sequence: the radical cations are scavenged by the nucleophile (eq 4); the resulting methoxy-substituted free radicals form simple methanol adducts (eq 5)[8] or generate more complex products by aromatic substitution at the ipso-carbon of the sensitizer radical anion (eq 6).[9]

$$\mathrm{Ph} \xrightarrow{h\nu} {}^1\mathrm{Ph}^* \quad (1)$$

$${}^1\mathrm{Ph}^* + \mathrm{DCB} \rightarrow \mathrm{Ph}^{\bullet+} + \mathrm{DCB}^{\bullet-} \quad (2)$$

$$\mathrm{Ph}^{\bullet+} + \mathrm{D} \rightarrow \mathrm{Ph} + \mathrm{D}^{\bullet+} \quad (3)$$

$$\mathrm{D}^{\bullet+} + \mathrm{CH_3OH} \rightarrow [\mathrm{D{-}OCH3}]^{\bullet} + \mathrm{H}^{+} \quad (4)$$

$$[\mathrm{D{-}OCH_3}]^{\bullet} \rightarrow\!\!\rightarrow \mathrm{H{-}D{-}OCH_3} \quad (5)$$

$$[\mathrm{D{-}OCH_3}]^{\bullet} + \mathrm{DCB}^{\bullet-} \rightarrow p\text{-}\mathrm{CN\text{-}C_6H_4{-}D{-}OCH_3} + \mathrm{CN}^{-} \quad (6)$$

Details of the reaction sequence leading to the three-component products are particularly well-established for olefins; this variant of the reaction is known as the photo-NOCAS reaction (for "photo-induced nucleophile-olefin-combination-aromatic-substitution").[9b,c] For the current study, the regiochemistry of nucleophilic attack on the radical cation ($\mathbf{3}^{\bullet+}$) is of primary interest. Accordingly, additional mechanistic details need not be delineated; however, some facets of individual reactions will emerge in the subsequent discussion.

The experimental findings are viewed in the light of *ab initio* calculations[10] on the prototype $\mathbf{1}^{\bullet+}$, the benzoannelated $\mathbf{2}^{\bullet+}$, and the bridged derivative $\mathbf{3}^{\bullet+}$. These species were calculated with the GAUSSIAN 94 electronic structure programs.[11] The extent of homoconjugation in these species will be based on the calculated geometries, especially the cyclopropane bond lengths, and on the carbon spin densities and hyperfine coupling parameters. Previous experience[12−15] suggests that this level of theory should reproduce the major geometric features of these systems.

Experimental Section

Materials and Solvents. The donor/substrate, tricyclo[4.3.1.0^{1,6}]-deca-2,4-diene (**3**) was prepared according to literature procedures.[7] The electron acceptor/sensitizers, 1,4-dicyanobenzene (Aldrich; 98%) and phenanthrene (Aldrich; 98%) were purified by recrystallization. 9,10-Dicyanoanthracene (Eastman Kodak) was purified by recrystallization from acetonitrile. Acetonitrile (Fischer), methanol (Fischer), and methylene chloride (Fischer; Spectranalyzed) were distilled from calcium hydride and stored over 4A molecular sieves in brown bottles under argon atmosphere.

Electron-Transfer Photosensitized Reactions. Solutions containing 0.1 M each of **3** and 1,4-dicyanobenzene and 0.02 M phenanthrene as co-sensitizer in acetonitrile/methanol (3:1) were deoxygenated by purging with argon for 15 min and irradiated in a Rayonet RPR-100 photoreactor equipped with 16 RPR-3500 lamps. The progress of the reaction was monitored by gas chromatography on a GC/MS system (HP 5890 series II GC interfaced with an HP 5971 mass selective detector), using a 12 m × 0.2 mm × 0.33 μm HP-1 capillary column (cross-linked methyl silicone on fused silica). Analytical runs were carried out in 4-mm i.d. NMR tubes stoppered with latex stoppers; preparative runs were in 30-mm i.d. tubes with central cooling fingers (water-cooling).

Isolation of Products. The major reaction products (>5% yield) were isolated by chromatography on a set of columns with IDs ranging from 1 to 5 cm, packed with ∼15 cm of TLC standard grade silica gel (Aldrich; without binder) and eluted with solvent gradients, usually from light petroleum ether (bp < 65 °C) to mixtures with either methylene chloride or ethyl acetate. Several passes were required to isolate the products.

Characterization of Products. Structure assignments of isolated products rest on MS and NMR data, including DEPT, two-dimensional COSY, and HETCOR experiments, where appropriate. NOE difference spectra were recorded to elucidate the substituent stereochemistry and the spatial relationship between the various functional groups. ^{1}H NMR spectra were recorded on either a Varian XL-400 or a Varian VXR-200 spectrometer. ^{13}C and HETCOR NMR spectra were recorded on a Varian VXR-200 spectrometer operating at 50.3 MHz.

Computational Details. *Ab initio* calculations[10] for norcaradienes, **1**−**3**, and their radical cations were carried out with the GAUSSIAN 94 series of electronic structure programs,[11] using extended basis sets, including d-type polarization functions on carbon (6-31G*). The geometries of the neutral parent molecules were optimized at the resticted Hartree−Fock level (RHF/6-31G*//RHF/6-31G*), those of radical cations were optimized at the unresticted Hartree−Fock level (UHF/6-31G*//UHF/6-31G*). Furthermore, the prototype, **1**, and its radical cation, $\mathbf{1}^{\bullet+}$, were also calculated to include higher degrees of electron correlation at the MP2 level of theory (MP2/6-31G*//MP2/6-31G*). Wave function analyses for charge and spin density distributions used the conventional Mulliken partitioning scheme.[10]

Møller−Plesset perturbation theory (UMP2) reproduces *positive* ^{1}H hyperfine coupling constants (hfcs) satisfactorily, but overestimates spin densities on carbon and negative hfcs significantly, often by factors >2.[12−15] On the other hand, density functional theory methods[16] give satisfactory agreement with experimental results.[16−18] Indeed, positive and negative hfcs of norbornadiene, quadricyclane, and bicyclobutane radical cations are reproduced accurately with either UB3LYP/6-31G*//UMP2/6-31G* or UB3LYP/6-31G*//UB3LYP/6-31G*.[18] Pictorial representations of spin density, SOMO and LUMO were derived with the program SPARTAN.[19] The previously optimized geometries (UMP2/6-31G* for $\mathbf{1}^{\bullet+}$, UHF/6-31G* for $\mathbf{2}^{\bullet+}$ and $\mathbf{3}^{\bullet+}$) were imported into SPARTAN. A UHF/6-31G* single-point calculation was followed by a surface analysis for spin density, SOMO and LUMO. In each case, the results are displayed as two separate views, containing translucent and opaque orbital outlines superimposed on the carbon frame.

(8) (a) Neunteufel, R. A.; Arnold, D. R. *J. Am. Chem. Soc.* **1973**, *95*, 4080. (b) Maroulis, A. J.; Shigemitsu, Y.; Arnold, D. R. *J. Am. Chem. Soc.* **1978**, *100*, 535. (c) Klett, M.; Johnson, R. P. *J. Am. Chem. Soc.* **1985**, *107*, 6615.

(9) (a) Rao, V. R.; Hixson, S. S. *J. Am. Chem. Soc.* **1979**, *101*, 6458. (b) Arnold, D. R.; Snow, M. S. *Can. J. Chem.* **1988**, *66*, 3012. (c) Arnold, D. R.; Du, X. J. *J. Am. Chem. Soc.* **1989**, *111*, 7666. (d) Arnold, D. R.; Du, X. *Can. J. Chem.* **1994**, *72*, 403.

(10) Hehre, W. J.; Radom, L.; Pople, J. A.; Schleyer, P. v. R. *Ab Initio Molecular Orbital Theory*; Wiley-Interscience: New York, 1986. This work presents a detailed description of the theoretical methods used in this work.

(11) Frisch, M. J.; Trucks, G. W.; Schlegel, H. B.; Gill, P. M. W.; Johnson, B. G.; Robb, M. A.; Cheeseman, J. R.; Keith, T.; Peterson, G. A. Montgomery, J. A.; Raghavachari, K.; Al-Laham, M. A.; Zakrzewski, V. G.; Ortiz, J. V.; Foresman, J. B.; Peng, C. Y.; Ayala, P. Y.; Chen, W.; Wong, M. W.; Andres, J. L.; Replogle, E. S.; Gomperts, R.; Martin, R. L.; Fox, D. J.; Binkley, J. S.; DeFrees, D. J.; Baker, J. P.; Stewart, J. P.; Head-Gordon, M.; Gonzalez, C.; Pople, J. A. *GAUSSIAN 94*; Gaussian, Inc., Pittsburgh, PA, 1994.

(12) Raghavachari, K.; Haddon, R. C.; Roth, H. D. *J. Am. Chem. Soc.* **1983**, *105*, 3110.

(13) Raghavachari, K.; Roth, H. D. *J. Am. Chem. Soc.* **1989**, *111*, 253.

(14) Roth, H. D.; Schilling, M. L. M.; Raghavachari, K. *J. Am. Chem. Soc.* **1984**, *106*, 253.

(15) Krogh-Jespersen, K.; Roth, H. D. *J. Am. Chem. Soc.* **1992**, *114*, 8388−8394.

(16) (a) Eriksson, L. A.; Malkin, V. G.; Malkina, O. L.; Salahub, D. R. *J. Chem. Phys.* **1993**, *99*, 9756−9763. (b) Eriksson, L. A.; Malkin, V. G.; Malkina, O. L.; Salahub, D. R. *Int. J. Quantum Chem.* **1994**, *52*, 879−901.

(17) Batra, R.; Giese, B.; Spichty, M.; Gescheidt, G.; Houk, K. N. *J. Phys. Chem.* **1996**, *100*, 18371−18379.

(18) Herbertz, T.; Roth, H. D. Unpublished results.

(19) SPARTAN, SGI Version 4.0.4 GL, Wavefunction Inc., 1991−1995, Irvine, CA. Deppmeier, B. J.; Driessen, A. J.; Hehre, W. J.; Johnson, H. C.; Leonard, J. M.; Yu, J.; Lou, L., Development Staff; Baker, J.; Carpenter, J. E.; Dixon, R. W.; Fielder, S. S.; Kahn, S. D.; Pietro, W. J., Contributors.

Results

The electron donor ability of tricyclo[4.3.1.0^{1,6}]deca-2,4-diene, **3**, was probed using the Stern−Volmer methodology; **3** is an efficient quencher of 9,10-dicyanoanthracene fluorescence. The Stern−Volmer plot is linear in the range, $10^{-2} < [\mathbf{3}] < 10^{-1}$ mol L^{-1}, $K_{SV} = \tau_f \times k_q = 220$; intercept 1.04 ± 0.01; and correlation coefficient > 0.9997. The value of the Stern−Volmer constant suggests quenching at an essentially diffusion controlled rate.

Irradiation of 1,4-dicyanobenzene/phenanthrene in an acetonitrile/methanol (3:1) solution containing **3** gave rise to two major NOCAS adducts, **4** and **5** (in yields of 27 and 24%; ∼75% conversion), and various minor methanol adducts (in ∼15% combined yield). Upon prolonged irradiation, two additional products, with a composition identical to that of NOCAS adducts, were formed in minor yields (<5% after >20 h of irradiation). Since these are clearly secondary products, and have no bearing on the reactivity of $\mathbf{3}^{\bullet+}$, they were not isolated. The methanol adducts were unstable and decomposed readily during attempts to isolate them.

The NMR spectra show that both NOCAS adducts contain an intact cyclopropane ring and one double bond; a methoxy and a cyanophenyl group have replaced one double bond in the six-membered ring. The integrity of the cyclopropane function is indicated by two ^{1}H doublets at 0.99 and 0.42 ppm for **4** and two closely overlapping resonances at ∼0.98 ppm for **5**, and by the corresponding ^{13}C resonances at 25.8 and 18.8 ppm, respectively, for **4** and **5**.

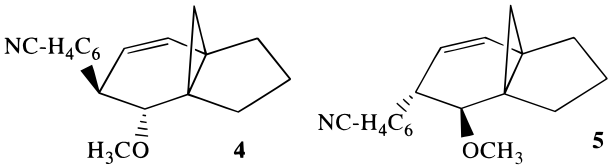

The structure assignment stands or falls with the correct identification of the tertiary ^{1}H resonances representing the protons adjacent to the newly introduced functionalities. Both products bear the methoxy and *p*-cyanophenyl functions on adjacent carbons since only one of their geminal protons shows a COSY cross-peak with the olefinic resonances. The identity of these resonances can be based on the HETCOR spectra because of the significant chemical shift difference between the ^{13}C resonances of tertiary alkoxy (88 and 87 ppm for **4** and **5**, respectively) and benzylic resonances (46 ppm for **4**, 47 ppm for **5**). The ^{1}H resonances (3.49 ppm) giving HETCOR cross-peaks with the less deshielded ^{13}C resonances show COSY cross-peaks with the olefinic signals; thus, the cyanophenyl groups occupy the position adjacent to both the alkene function and the carbon bearing the methoxy group.

The orientation of the two substituents with respect to the cyclopropane moiety and relative to each other rests on ^{1}H chemical shift and NOE arguments. The orientation of the aryl group in adduct **4** is based on the substantial difference between the chemical shifts of the two cyclopropane protons (H_{anti} 0.99 ppm, H_{syn} 0.42 ppm; $\Delta\delta = 0.57$). Since the geminal cyclopropane protons of the isomer **5** and of the parent bicyclo[4.1.0]-hept-2-ene (norcarene) have much less divergent chemical shifts, the additional shielding of one resonance in **4** is ascribed to the shielding effect of the aryl group. This assignment requires that the aryl group occupies the position cis to the cyclopropane ring. The orientation of the methoxy group of **4** is based on the NOE enhancement (intermediate intensity) of the tertiary alkoxy resonance (H_5) upon preirradiating the more highly deshielded cyclopropane resonance. This result suggests that H_5 lies cis and, accordingly, the methoxy group lies trans to the cyclopropane ring.

The cyclopropane resonances (0.98 ppm) of the second isomer (**5**) are not resolved; this is compatible with an aryl group anti to the cyclopropane ring. The 2D COSY spectrum reveals a small coupling between the tertiary alkoxy proton (3.37 ppm) and the cyclopropane resonance (0.98 ppm), typical for norbornene protons in a W-type relationship.[20] Accordingly, the tertiary alkoxy resonance is assigned the endo geometry. This conclusion is further supported by NOE experiments. Preirradiation of the cyclopropane resonance (0.98 ppm) caused strong NOE enhancement for the methoxy signal and weaker enhancement for a resonance at 1.7 ppm, which is part of the trimethylene bridge spectrum. Furthermore, MM3 calculations show the preferred conformer of **5** as having a nearly anti-trans arrangement of the two tertiary protons, H_2 and H_3, of the six-membered ring, in line with the large *J* coupling (9.0 Hz) observed for the corresponding resonances.

Discussion

The potential homoconjugation between the butadiene and cyclopropane moieties in norcaradiene radical cations is of interest since it may favor an interesting and uncommon electronic state of cyclopropane radical cation.[21] Cyclopropane has a degenerate pair of in-plane e′ orbitals (*S*, *A*) whose vertical ionization leads to a doubly degenerate ^{2}E′ state. Jahn−Teller (JT) distortion of this state results in two nondegenerate electronic states, $^2A_1$ and $^2B_2$ (C_{2v} symmetry).[21,22] The $^2A_1$ component (orbital *S* singly occupied) relaxes to an equilibrium structure with one lengthened C−C bond, which is the lowest energy species for many cyclopropane radical cations, as based on ESR[23,24] or CIDNP spectroscopic studies.[6]

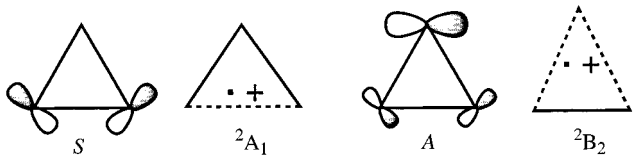

The interaction with the butadiene frontier molecular orbital (FMO) may lift the degeneracy of the cyclopropane in-plane e′ orbitals (*S*, *A*) and favor the $^2B_2$ component. This conclusion follows from an approach based on FMO/perturbational (P) MO theory.[25,26] The substrates are dissected into molecular fragments and the potential interactions of the component FMOs are considered. According to PMO theory,[25] the strength of

(20) Marchand, A. P. *Stereochemical Applications of NMR Studies in Rigid Bicyclic Systems*; Verlag Chemie International: Deerfield Beach, 1982; Chapter 4.

(21) (a) Haselbach, E. *Chem. Phys. Lett.* **1970**, *7*, 428. (b) Rowland, C. G. *Chem. Phys. Lett.* **1971**, *9*, 169. (c) Collins, J. R.; Gallup, G. A. *J. Am. Chem. Soc.* **1982**, *104*, 1530. (d) Bouma, W. J.; Poppinger, D.; Radom, L. *Isr. J. Chem.* **1983**, *23*, 21. (e) Wayner, D. D. M.; Boyd, R. J.; Arnold, D. R. *Can. J. Chem.* **1985**, *63*, 3283. (f) Wayner, D. D. M.; Boyd, R. J.; Arnold, D. R. *Can. J. Chem.* **1983**, *61*, 2310. (g) Du, P.; Hrovat, D. A.; Borden, W. T. *J. Am. Chem. Soc.* **1988**, *110*, 3405.

(22) (a) Jahn, H. A.; Teller, E. *Proc. R. Soc. London, Ser. A.* **1937**, *161*, 220. (b) Pearson, R. G. *J. Am. Chem. Soc.* **1969**, *91*, 4947. (c) Opik, U.; Pryce, M. H. L. *Proc. R. Soc. London, Ser. A.* **1957**, *238*, 425.

(23) Iwasaki, M.; Toriyama, K.; Nunome, K. *J. Chem. Soc. Chem. Commun.* **1983**, 202.

(24) (a) Qin, X. Z.; Snow, L. D.; Williams, F. *J. Am. Chem. Soc.* **1984**, *106*, 7640. (b) Qin, X. Z.; Williams, F. *Tetrahedron* **1986**, *42*, 6301.

(25) Dewar, M. J. S.; Dougherty, R. C. *The PMO Theory of Organic Chemistry*; Plenum Press: New York, 1975.

(26) Haddon, R. C.; Roth, H. D. *Croat. Chem. Acta* **1984**, *57*, 1165−1176.

the fragment perturbation is approximately proportional to $S^2/\Delta E$, where S is the overlap integral between the components and ΔE is the difference between the FMO energies; the S^2 term will depend on factors, such as the FMO symmetry, the magnitude of the coefficients at the points of union, and the orientation of the fragments.[26] Although the FMO energies of butadiene ($I = 9.1$ eV)[27] and cyclopropane ($I = 10.1$ eV)[28] are not optimally matched, the overlap integral may be favorable: the orbital symmetry of the butadiene FMO matches that of the cyclopropane *A* orbital, the coefficients at the points of union are significant, and the orientation of the fragments should permit overlap. As a result, two new "molecular" orbitals are generated by symmetrical and antisymmetrical combination of the two FMOs.

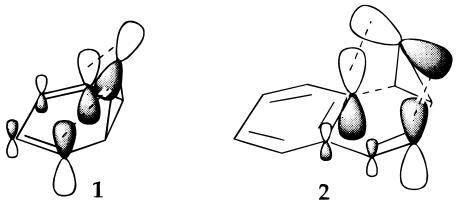

1 **2**

The experimental approach is based on the assumption that the nucleophile, methanol, will add to carbons for which the singly occupied molecular orbital (SOMO) has significant orbital coefficients. The structure(s) of the resulting products designate the regiochemistry of nucleophilic attack and, possibly, may reveal the extent of homoconjugation between the interacting cyclopropane and olefinic functionalities. At the same time, the stereochemical features of the products delineate the stereochemistry of nucleophilic capture by the radical cation (eq 4) and of aromatic substitution by the adduct free radical (eq 6).

***Ab Initio* Calculations.** A complementary approach to evaluate the extent of homoconjugation in the radical cations $\mathbf{1}^{\bullet+}-\mathbf{3}^{\bullet+}$ involves *ab initio* calculations. All calculations employed the 6-31G* basis set for geometry optimizations and single-point calculations. The geometry of prototype, $\mathbf{1}^{\bullet+}$, was optimized with the unrestricted Hartree−Fock (UHF), Becke hybrid (UB3LYP), and Møller−Plesset (UMP2) methods, followed in each case by a standard population analysis. The geometries obtained from the HF and MP2 optimization were also subjected to a UB3LYP single-point calculation. For the radical cations, $\mathbf{2}^{\bullet+}$ and $\mathbf{3}^{\bullet+}$, standard UHF optimizations and population analysis were performed in addition to a UB3LYP single point calculation. The structures of radical cations, $\mathbf{1}^{\bullet+}-\mathbf{3}^{\bullet+}$, will be discussed in terms of the calculated geometries (at the UMP2 level for $\mathbf{1}^{\bullet+}$, at the UHF level for $\mathbf{2}^{\bullet+}$ and $\mathbf{3}^{\bullet+}$), the spin densities and hfcs derived from single-point calculations (at the UB3LYP level), and SOMO, LUMO, and spin density surface visualizations produced with SPARTAN. The UB3LYP wave functions have only a small spin contamination, $S^2 \approx 0.76$ (vide infra).

Norcaradiene Radical Cation. The radical cation, $\mathbf{1}^{\bullet+}$, has a $^2A''$ electronic state and C_s symmetry; the minimization converges to this symmetry, regardless of whether symmetry is imposed or not. The C−C bond distances between the cyclopropane carbons are very similar, the internal bond ($C_1-C_6 = 153.8$ pm) being slightly longer than that of the two lateral bonds ($C_1-C_7 = C_6-C_7 = 153.3$ pm). The bonds connecting the cyclopropane and butadiene moieties ($C_1-C_2 = C_5-C_6 = 143.1$ pm) are of intermediate length; finally, the bonds between the two pairs of olefinic carbons ($C_2-C_3 = C_4-C_5 = 139.5$ pm) are only marginally longer than that of the intervening bond ($C_3-C_4 = 140.5$ pm), not unexpected for a butadiene radical cation. These bond lengths (Table 1) appear to offer limited insight concerning homoconjugation.

Table 1. Bond Lengths (pm) of Norcaradiene (1) and Its Radical Cation

		$\mathbf{1}^{\bullet+}$		
bond	**1** RMP2//RMP2	UHF// UHF	UB3LYP// UB3LYP	UMP2// UMP2
C_1-C_2	146.2	145.8	144.8	143.1
C_2-C_3	136.2	138.9	139.4	139.5
C_3-C_4	145.8	139.3	141.0	140.5
C_1-C_6	157.2	152.1	152.6	153.8
C_1-C_7	150.2	151.0	154.2	153.3

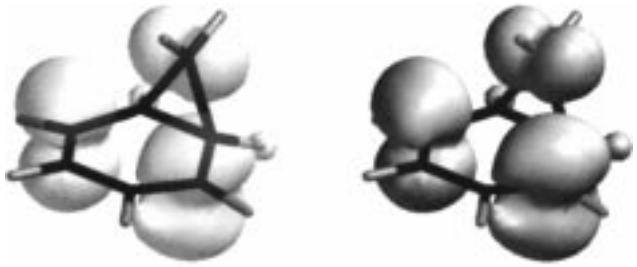

Figure 1. Pictorial representation of the spin density distribution of norcaradiene radical cation calculated with Spartan.[19]

Table 2. Spin Density Distribution of Norcaradiene Radical Cation, $\mathbf{1}^{\bullet+}$

$\mathbf{1}^{\bullet+}$	UHF// UHF ($S^2 = 0.85$)	UB3LYP// UHF ($S^2 = 0.76$)	UB3LYP// UB3LYP ($S^2 = 0.759$)	UB3LYP// UMP2 ($S^2 = 0.759$)	UMP2// UMP2 ($S^2 = 0.845$)
C_1	−0.090	−0.016	−0.015	−0.012	−0.095
C_2	0.610	0.370	0.346	0.359	0.594
C_3	−0.034	0.090	0.095	0.090	−0.029
C_7	0.231	0.210	0.255	0.246	0.289

The carbon spin density distribution documents the presence of spin on C_7 and, thus, clearly supports the type of homoconjugation suggested by simple qualitative FMO considerations. Although the spin density at C_7 ($\rho_7 = 0.246$) is lower than that at the terminal butadiene carbons, ($\rho_{2,5} = 0.359$), the delocalization of spin and charge onto C_7 supports a structure type related to the $^2B_2$ radical cation of cyclopropane (Figure 1). However, it is noteworthy that the extent of delocalization depends significantly on the level of perturbation theory included (Table 2). Thus, calculations at the UHF level show significantly less delocalization ($\rho_{2,5} = 0.61$, $\rho_7 = 0.231$) than is revealed by second-order Møller−Plesset perturbation theory (UMP2).

Not surprisingly, the structure type derived by considering the spin density distribution is also fully revealed in the hyperfine coupling pattern. Two olefinic protons (H_2 and H_5) and the two geminal cyclopropane protons show significant negative hfcs ($a_{2,5} = -9.1$ G; $a_{7\text{syn}} = -5.7$ G; $a_{7\text{anti}} = -6.3$ G); the bridgehead carbons show sizable positive hfcs ($a_{1,6} = 13.6$ G); finally, the olefinic protons near the node show negligible hfcs ($a_{3,4} = -0.4$ G). Again, the degree of delocalization depends on the level of perturbation theory (Table 3). At the UHF level, the olefinic coupling is slightly larger ($a_{2,5} = -22.1$ G), whereas the geminal cyclopropane couplings are smaller ($a_{7\text{syn}} = -8.0$ G; $a_{7\text{anti}} = -7.0$ G) than those calculated with second-order Møller−Plesset theory.

(27) Bieri, G.; Burger, F.; Heilbronner, E.; Meier, J. P. *Helv. Chim. Acta* **1977**, *60*, 2213.

(28) Basch, H.; Robin, M. B.; Kuebler, N. A.; Baker, C.; Turner, D. W. *J. Chem. Phys.* **1969**, *51*, 52.

Table 3. Calculated Hyperfine Coupling Constants of Norcaradiene Radical Cation

$1^{\bullet+}$	UHF// UHF ($S^2 = 0.85$)	UB3LYP// UHF ($S^2 = 0.76$)	UB3LYP// UB3LYP ($S^2 = 0.759$)	UB3LYP// UMP2 ($S^2 = 0.759$)	UMP2// UMP2 ($S^2 = 0.845$)
H_1	13.1	14.9	15.0	13.6	12.9
H_2	−22.1	−9.3	−8.5	−9.1	−21.6
H_3	−0.2	−2.6	−2.9	−2.5	−0.4
H_{7s}	−8.0	−5.0	−6.0	−5.7	−9.8
H_{7a}	−7.0	−5.4	−6.5	−6.3	−8.9

Table 4. Bond Lengths (pm) of Norcaradiene Derivatives and Their Radical Cations

bond	**2** RHF//RHF	$\mathbf{2}^{\bullet+}$ UHF//UHF	bond	**3** RHF//RHF	$\mathbf{3}^{\bullet+}$ UHF//UHF
C_1-C_2	148.4	145.4			
			C_1-C_2	148.2	145.2
C_5-C_6	149.2	148.5			
C_2-C_3	132.5	138.5			
			C_2-C_3	132.9	139.3
C_4-C_5	140.0	143.8			
C_3-C_4	147.2	139.9	C_3-C_4	146.9	139.1
C_1-C_6	151.2	151.3	C_1-C_6	153.0	153.9
C_1-C_7	150.1	152.4			
			C_1-C_{10}	149.9	150.8
C_6-C_7	150.0	149.1			

Table 5. Spin Density Distribution of Radical Cations $\mathbf{2}^{\bullet+}$ and $\mathbf{3}^{\bullet+}$

$\mathbf{2}^{\bullet+}$	UHF// UHF ($S^2 = 1.146$)	UB3LYP// UHF ($S^2 = 0.762$)	$\mathbf{3}^{\bullet+}$	UHF// UHF ($S^2 = 0.842$)	UB3LYP// UHF ($S^2 = 0.76$)
C_1	−0.074	−0.009			
			C_1	−0.096	−0.022
C_6	−0.081	−0.007			
C_2	0.567	0.355			
			C_2	0.619	0.383
C_5	0.621	0.153			
C_3	−0.002	0.097			
			C_3	−0.029	0.087
C_4	−0.109	0.134			
C_7	0.183	0.149	C_{10}	0.215	0.203
			C_7	0.021	0.024

Benzobicyclo[4.1.0]hepta-2,4-diene Radical Cation. Radical cation, $\mathbf{2}^{\bullet+}$, was optimized at the UHF/6-31G* level of theory; $\mathbf{2}^{\bullet+}$ has no symmetry. The cyclopropane C−C bonds show subtle differences (Table 4); the lateral bond conjugated with the ethene function ($C_1-C_7 = 152.4$ pm) is longer, whereas that conjugated with the benzene ring is shorter ($C_6-C_7 = 149.1$ pm), than the internal bond ($C_1-C_6 = 151.3$ pm). The bonds linking the strained ring to the styrene moiety are slightly longer ($C_1-C_2 = 145.4$ pm; $C_5-C_6 = 148.5$ pm) than those of the styrene function ($C_2-C_3 = 138.5$ pm; $C_4-C_5 = 143.8$ pm; $C_3-C_4 = 139.9$ pm).

The calculated carbon spin densities of the radical cation nicely document the extent of homoconjugation (Table 5); most of the spin is located on C_2 ($\rho_2 = 0.355$), significantly less on C_5 and C_7 ($\rho_5 = 0.153$, $\rho_7 = 0.149$), whereas the tertiary cyclopropane carbons, C_1 and C_6 ($\rho_1 = -0.009$, $\rho_6 = -0.007$), have essentially no spin density (Figure 2). The calculated hfcs (Table 6) are in good qualitative agreement with the CIDNP effects observed during the electron transfer from benzonorcaradiene, **2**, to photoexcited chloranil.[6] The tertiary cyclopropane ^{1}H nuclei, H_1 and H_6, have large positive hfcs ($a_1 = 9.3$ G, $a_6 = 10.6$ G), whereas the geminal cyclopropane nuclei ($H_{7s,a}$) have negative hfcs of moderate magnitude ($a_{7s} = -3.4$ G, $a_{7a} = -2.8$ G).

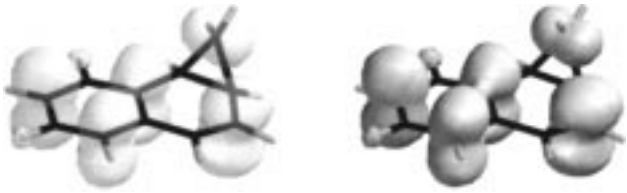

Figure 2. Pictorial representation of the spin density distribution of benzonorcaradiene radical cation calculated with Spartan.

Table 6. Comparison of ^{1}H CIDNP Effects with Hyperfine Coupling Constants[a]

benzonorcaradiene				tricyclo[4.3.1.0]decadiene		
	CIDNP[b]	UHF// UHF[a] ($S^2 = 1.146$)	UB3LYP// UHF[a] ($S^2 = 0.762$)		UHF// UHF[a] ($S^2 = 0.842$)	UB3LYP// UHF[a] ($S^2 = 0.76$)
H_1	m E	9.2	9.3			
H_2	m A	−20.6	−8.7	H_2	−22.0	−9.6
H_3	m A	−0.5	−2.7	H_3	−0.6	−2.5
H_6	s E	9.7	10.6			
H_{7s}	m A	−6.1	−3.4	H_{10s}	−7.6	−5.4
H_{7a}	m A	−3.6	−2.8	H_{10a}	−6.8	−4.8
				H_{7s}	−1.8	−1.1
				H_{7a}	−0.8	0.8

[a] Hyperfine coupling constants in Gauss. [b] E, emission; A, enhanced absorption; s, strong; m, medium. Under the conditions of the CIDNP experiment,[6] ^{1}H nuclei with positive hfcs are expected in emission, whereas ^{1}H nuclei with negative hfcs will show enhanced absorption.

Figure 3. Pictorial representation of the spin density distribution of tricyclo[4.3.1.0]decadiene radical cation calculated with Spartan.

Tricyclo[4.3.1.0^{1,6}]deca-2,4-diene Radical Cation. The radical cation, $\mathbf{3}^{\bullet+}$, was optimized at the UHF/6-31G* level of theory with imposed C_s symmetry; this species also has a ^{2}A″ electronic state. The C−C bond distances (Table 4) between the cyclopropane carbons are slightly more divergent than those found for $\mathbf{1}^{\bullet+}$, the internal bond ($C_1-C_6 = 153.9$ pm) being 3 pm longer than the two lateral bonds ($C_1-C_{10} = C_6-C_{10} = 150.8$ pm). The bonds connecting the cyclopropane and butadiene moieties ($C_1-C_2 = C_5-C_6 = 145.2$ pm) are longer than the corresponding bonds of $\mathbf{1}^{\bullet+}$; finally, the bonds between the two pairs of olefinic carbons ($C_2-C_3 = C_4-C_5 = 139.3$ pm) have essentially the same length as the intervening bond ($C_3-C_4 = 139.1$ pm).

The carbon spin density on the bridge carbon is lower than that calculated for $\mathbf{1}^{\bullet+}$ ($\rho_{10} = 0.203$), even considering the lower level of theory (Table 5); correspondingly, the terminal butadiene carbons have slightly higher spin densities ($\rho_{2,5} = 0.383$; Figure 3). The hyperfine coupling pattern of $\mathbf{3}^{\bullet+}$ shows corresponding minor changes relative to $\mathbf{1}^{\bullet+}$ (Table 6): increased hfcs for the olefinic protons $H_{2,5}$ ($a_{2,5} = -9.6$ G) and decreased hfcs for the cyclopropane protons ($a_{10syn} = -5.4$ G; $a_{10anti} = -4.8$ G). In summary, these data again support a structure type related to the $^2B_2$ prototype radical cation of cyclopropane; the degree of homoconjugation, as judged by the extent of delocalization, is somewhat less than found for $\mathbf{1}^{\bullet+}$. This difference may be a consequence of the trimethylene bridge; although this feature is instrumental in stabilizing the norcaradiene structure, it may limit somewhat the extent of homoconjugation due to

steric factors. Still, the calculations predict a significant role of homoconjugation in the radical cations, $\mathbf{1}^{\bullet+}$ and $\mathbf{3}^{\bullet+}$, encouraging the pursuit of this problem by experimental methods.

Electron-Transfer Photochemistry of Norcaradiene (3). The photoinduced electron-transfer reaction of **3** with 1,4-dicyanobenzene and phenanthrene in acetonitrile−methanol generates NOCAS products **4** and **5** as the major products. The electron-transfer generating the radical ion pair, $\mathbf{3}^{\bullet+}$−$\mathbf{DCB}^{\bullet-}$ (cf., eqs 1−3), is exergonic.[29] The radical cation, $\mathbf{3}^{\bullet+}$, is formed by an indirect pathway; singlet excited phenanthrene, $^1\mathbf{Ph}^*$ (Ph, $E_{0,0} = 3.58$ eV, $E_{(D/D+)} = 1.58$ V),[31] is quenched by electron transfer to 1,4-dicyanobenzene ($E_{(A^-/A)} = -1.60$ V;[31] $\Delta G = -0.34$ eV); a second electron transfer from **3** ($E_{(D/D+)} = \sim 1.0$ V)[32] to $\mathbf{Ph}^{\bullet+}$ generates $\mathbf{3}^{\bullet+}$. Thus, the products are plausibly explained by a mechanism involving electron transfer followed by the capture of $\mathbf{3}^{\bullet+}$ by methanol. The fact that all products contain the methoxy group, underscores the importance of nucleophilic capture as a primary radical cation reaction (cf., eq 4).

The position of the methoxy groups in the products identifies the position of attack and delineates the approach of methanol from the face syn or anti to the cyclopropane ring. The products are formed in regiospecific fashion (capture at C_2, C_5), but with limited stereoselectivity. Since products **4** and **5** are formed in comparable yields, the barriers for *syn*- or *anti*-attack must be comparable.

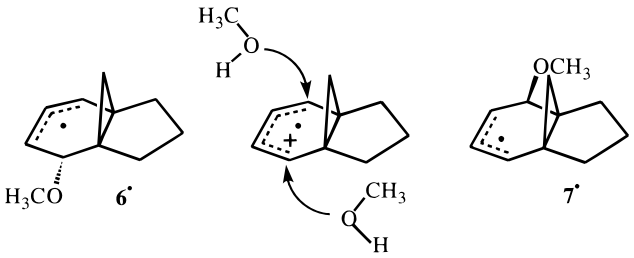

Interestingly, no products are derived by nucleophilic attack on the cyclopropane ring of $\mathbf{3}^{\bullet+}$, even though *ab initio* calculations suggest that spin (and charge) are delocalized onto the strained ring, notably onto C_{10} (vide supra). Contrary to ample precedent suggesting release of strain as an important principle in radical cation reactions,[35−37] particularly when leading to delocalized free-radicals, viz., $\mathbf{8}^{\bullet}$ or $\mathbf{9}^{\bullet}$, $\mathbf{3}^{\bullet+}$ fails to follow this reactivity pattern.

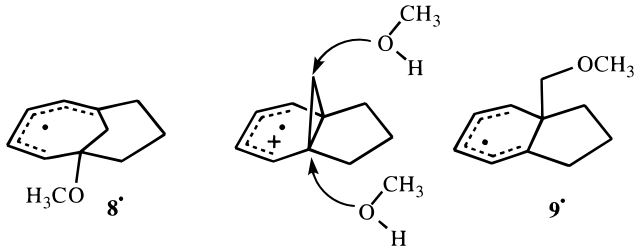

Although the relative energies of the four potential products of nucleophilic capture appear straightforward, we also calculated the free energies of the free radicals ($\mathbf{10}^{\bullet}$−$\mathbf{13}^{\bullet}$) derived by nucleophilic capture of the (truncated) parent system ($\mathbf{1}^{\bullet+}$) to probe the assumed gradation of relative energies. The results (at the UHF/6-31G* level of theory) unambiguously confirm the expected relative energies and elucidate additional details. The *syn*- or *anti*-methoxynorcarenyl radicals have essentially identical energies and lie substanticantly above the ring-opened free radicals, methoxycycloheptadienyl ($\mathbf{12}^{\bullet}$) and methoxymethylcyclohexadienyl ($\mathbf{13}^{\bullet}$).

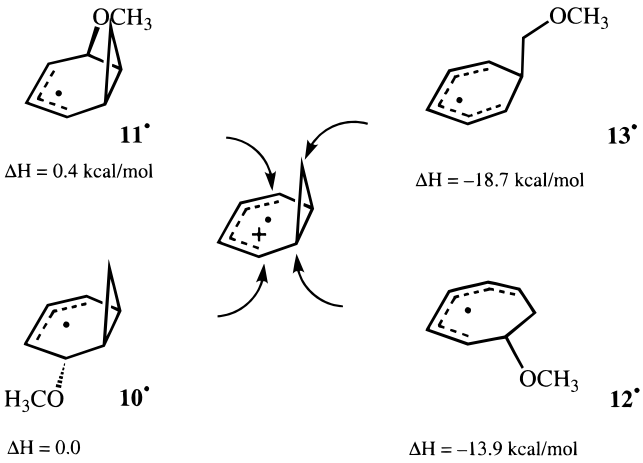

The obvious failure to form the more stable ring-opened products leads us to consider the factors affecting the stereo- and regiochemistry of radical cation nucleophilic capture. Experimental results support several governing factors, including the following: (1) the spin and charge density distribution in the radical cation (educt); (2) the extent of conjugation in educt and free-radical product; (3) the release of ring strain upon forming the product. Steric factors are not expected to play a major role; in fact, several radical cations have been captured by attack on highly congested centers.[37a,b] Finally, the selectivity (reactivity) of the nucleophile may play a role; a nucleophile of limited selectivity is needed if it is to attack centers of secondary spin and charge density. Methanol is a selective reagent: it attacks $\mathbf{3}^{\bullet+}$ in highly regiospecific fashion and captures the β-phellandrene radical cation, $\mathbf{14}^{\bullet+}$, with high regiospecificity at the *exo*-methylene carbon and the sabinene radical cation, $\mathbf{15}^{\bullet+}$, exclusively at the quaternary carbon.[37a,b]

The spin and charge density distribution of the radical cation is an obvious (perhaps trivial) consideration, as it delineates the singly occupied molecular orbital (SOMO), which must be involved in the reaction. This consideration eliminates the attack at C_1/C_6 (leading to $\mathbf{8}^{\bullet}$) as a viable reaction, because the bridgehead carbons are nodal centers; however, attack at C_{10}

(29) The free energy of radical ion pair formation was calculated according to the Rehm−Weller equation: $-\Delta G = E_{(0,0)} - E_{(D/D+)} + E_{(A^-/A)} + e^2/\epsilon a$.[30]

(30) (a) Knibbe, H.; Rehm, D.; Weller, A. *Ber. Bunsen-Ges. Phys. Chem.* **1968**, *72*, 257. (b) Weller, A. *Pure Appl. Chem.* **1968**, *16*, 115. (c) Rehm, D.; Weller, A. *Isr. J. Chem.* **1970**, *8*, 259.

(31) Mattes, S. L.; Farid, S. *Org. Photochem.* **1983**, *6*, 233.

(32) The oxidation potential of **3** is estimated to lie below those of 2-carene ($E_{(D/D+)}$ +1.39 V)[33a] and cyclohexa-1,3-diene ($E_{(D/D+)}$ +1.35 V).[33b] The Stern−Volmer constant for quenching 9,10-dicyanoanthracene fluorescence by **3** is similar to that of quadricyclane ($E_{(D/D+)} = 0.91$ V)[34.]

(33) (a) Arnold, D. R.; Du, X.; de Lijser, H. J. P. *Can. J. Chem.* **1995**, *73*, 522. (b) Kubo, Y.; Suto, M.; Araki, T. *J. Org. Chem.* **1986**, *51*, 4404−4411.

(34) Gassman, P. G.; Olson, K. D.; Walter, L.; Yamaguchi, R. *J. Am. Chem. Soc.* **1979**, *101*, 1308.

(35) (a) Rao, V. R.; Hixson, S. S. *J. Am. Chem. Soc.* **1979**, *101*, 6458. (b) Mizuno, K.; Ogawa, J.; Kagano, H.; Otsuji, Y. *Chem. Lett.* **1981**, 437. (c) Mizuno, K.; Ogawa, J.; Otsuji, Y. *Chem. Lett.* **1981**, 741. (d) Hixson, S. S.; Xing, Y. *Tetrahedron Lett.* **1991**, *32*, 173−174.

(36) (a) Gassman, P. G.; Olson, K. D.; Walter, L.; Yamaguchi, R. *J. Am. Chem. Soc.* **1981**, *103*, 4977. (b) Gassman, P. G.; Olson, K. D. *J. Am. Chem. Soc.* **1982**, *104*, 3740.

(37) (a) Weng, H.; Sethuraman, V.; Roth, H. D. *J. Am. Chem. Soc.* **1994**, *116*, 7021−7025. (b) Weng, H.; Sheik, Q.; Roth, H. D. *J. Am. Chem. Soc.* **1995**, *117*, 10655−10661. (c) Herbertz, T.; Roth, H. D. *J. Am. Chem. Soc.* **1996**, *118*, 10954−10962.

Figure 4. Spartan representation of SOMO (bottom) and LUMO (top) for norcaradiene radical cation, $\mathbf{1}^{\bullet+}$.

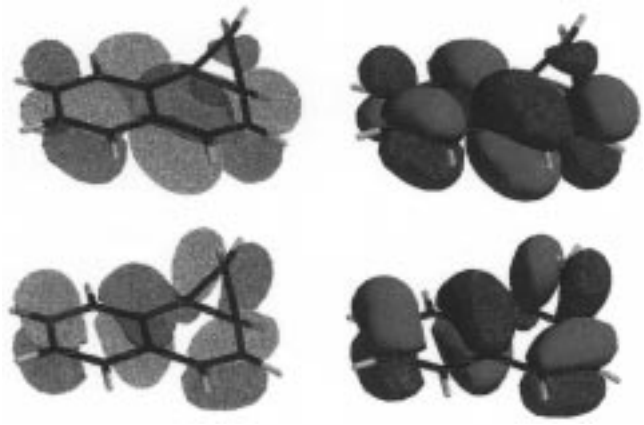

Figure 5. Spartan representation of SOMO (bottom) and LUMO (top) for benzonorcaradiene radical cation, $\mathbf{2}^{\bullet+}$.

(leading to $\mathbf{9}^{\bullet}$) remains feasible. Two other factors, release of ring strain (vide supra) and delocalization of the unpaired spin in the newly formed free-radicals, are of major importance in many reactions. For example, $\mathbf{15}^{\bullet+}$ generates a conjugated radical cation, $\mathbf{14}^{\bullet+}$, via a sigmatropic shift, and an allyl radical, $\mathbf{16}^{\bullet}$, upon nucleophilic attack.[37] Both reactions form fully conjugated "products" with full relief of ring strain. Similarly, nucleophilic attack on 1-aryl-2-alkylcyclopropanes forms benzyl radicals;[38] attack on styrene radical cations also forms delocalized (benzyl) radicals exclusively.[39] These considerations still leave attack at C_{10} as an option.

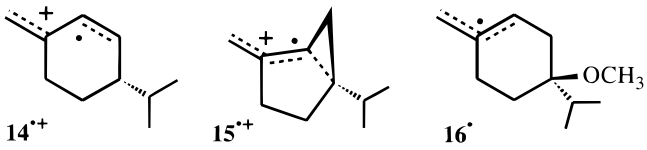

None of these factors can explain the absence of products formed with relief of ring strain, i.e., the failure of $\mathbf{3}^{\bullet+}$ to undergo nucleophilic capture at the strained ring. The key to this observation may lie in the nature of the high lying orbitals of $\mathbf{3}^{\bullet+}$, which may be involved in the reaction, i.e., its SOMO and

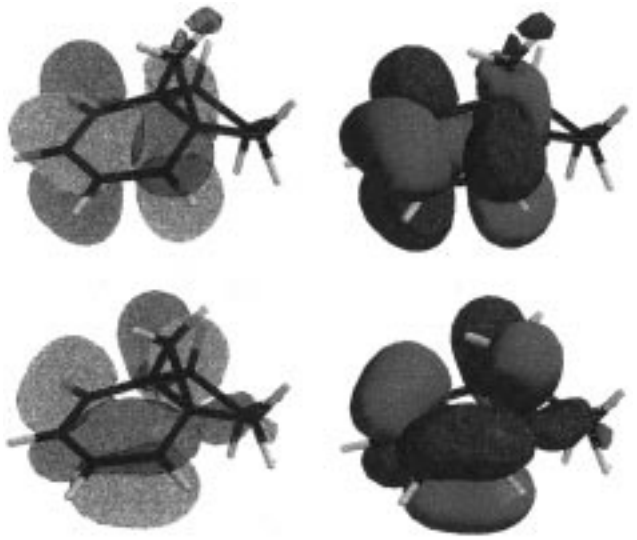

Figure 6. Spartan representation of SOMO (bottom) and LUMO (top) for tricyclo[4.3.1.0]decadiene radical cation, $\mathbf{3}^{\bullet+}$.

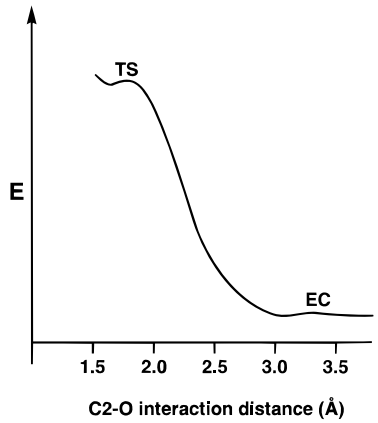

Figure 7. Reaction profile for the capture of norcaradiene radical cation, $\mathbf{1}^{\bullet+}$, by methanol.

LUMO. This approach has precedent in several theoretical treatments. Pross probed the capture of radical cations by nucleophiles with curve crossing methodologies. The excited state in the curve crossing involves "double excitation";[40] later, Shaik and Pross showed that the excitation energy may be small and the resulting barrier low.[41] This prediction was confirmed by results of Eberson and co-workers; nucleophiles attack dibenzofuran radical cation at the site of the highest LUMO coefficient, which coincides with the site of highest spin density in the dibenzofuran triplet state.[42] Similarly, Shaik and collaborators explained the well-documented stereochemical course of nucleophilic displacement of a σ bond (with inversion of configuration)[4,36−38,43] by involvement of the σ^* orbital (the LUMO) of the weakened bond.[44]

(38) (a) Dinnocenzo, J. P.; Todd, W. P.; Simpson, T. R.; Gould, I. R. *J. Am. Chem. Soc.* **1990**, *112*, 2462. (b) Dinnocenzo, J. P.; Lieberman, D. R.; Simpson, T. R. *J. Am. Chem. Soc.* **1993**, *115*, 366−367. (c) Dinnocenzo, J. P.; Simpson, T. R.; Zuilhof, H.; Todd, W. P.; Heinrich, T. *J. Am. Chem. Soc.* **1997**, *119*, 987−993. (d) Dinnocenzo, J. P.; Zuilhof, H.; Lieberman, D. R.; Simpson, T. R.; McKechney, M. W. *J. Am. Chem. Soc.* **1997**, *119*, 994−1004.

(39) Arnold, D. R.; Humphreys, R. W. R. *J. Am. Chem. Soc.* **1979**, *101*, 2743.

(40) Pross, A. *J. Am. Chem. Soc.* **1986**, *108*, 3537.

(41) Shaik, S. S.; Pross, A. *J. Am. Chem. Soc.* **1989**, *111*, 4306.

(42) (a) Eberson, L.; Radner, F. *Acta Chem. Scand.* **1992**, *46*, 312. (b) Eberson, L.; Radner, F. *Acta Chem. Scand.* **1992**, *46*, 802. (c) Eberson, L.; Hartshorn, M. P.; Radner, F.; Merchan, M.; Roos, B. O. *Acta Chem. Scand.* **1993**, *47*, 176.

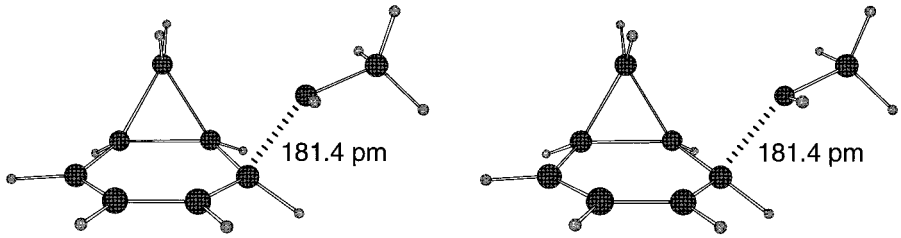

Figure 8. Transition state (stereoview) for the nucleophilic capture of $\mathbf{1}^{\bullet+}$ by methanol in syn fashion.

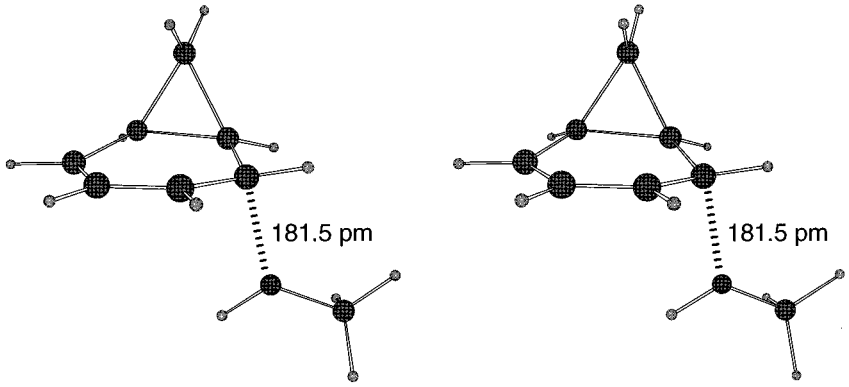

Figure 9. Transition state (stereoview) for the nucleophilic capture of $\mathbf{1}^{\bullet+}$ by methanol in anti fashion.

We propose that the norcaradiene radical cation, $\mathbf{1}^{\bullet+}$, or the bridged derivative, $\mathbf{3}^{\bullet+}$, are exceedingly well suited to probe the principles governing the nucleophilic capture of radical cations. This becomes evident when considering the combined effects due to free energy and molecular orbital contributions. We have mentioned the significant free energy differences between attack at the strained ring (yielding $\mathbf{8}^{\bullet}$ and $\mathbf{9}^{\bullet}$) and addition to the diene moiety (giving rise to $\mathbf{6}^{\bullet}$ and $\mathbf{7}^{\bullet}$). Perhaps more importantly, the two MOs potentially involved in the reaction have a substantially different distribution of orbital coefficients. The SOMOs of $\mathbf{1}^{\bullet+}$ and $\mathbf{3}^{\bullet+}$ show large orbital coefficients at $C_{2,5}$ and C_7 (C_{10}), which are reflected in the hyperfine pattern of these species (Figures 4 and 6, bottom). In contrast, the principal orbital coefficients of the LUMOs are located at $C_{2,5}$ and $C_{3,4}$. Most importantly, the orbital lobes at C_7 (C_{10}) offer no target for an attack by the nucleophile (Figures 4 and 6, top). Because of the differing orbital coefficients of SOMO and LUMO, the norcaradiene system will elucidate whether the regioselectivity of nucleophilic capture is governed by the spin density, i.e., the SOMO, or whether the nature and topology of the LUMO are also significant. The products derived from $\mathbf{3}^{\bullet+}$ are clearly formed by attack at a center where both SOMO and LUMO have significant orbital coefficients. This assignment is all the more persuasive as the reaction of $\mathbf{3}^{\bullet+}$ fails to follow the direction of a significant advantage in driving force. The special significance of the system introduced here lies in the fact that MO arguments and free energy considerations predict a different regioselectivity. Apparently, the molecular orbital requirements outweigh the significant free energy differences due to the relief of ring strain and extended conjugation.

Additional support for this assignment is provided by calculations modeling the approach of methanol to norcaradiene radical cation. At the UHF/6-31G* level of theory (which models the nucleophilic attack in the gas phase), the reaction profile for the attack on the terminal butadiene carbons (C_2, C_5) has two separate saddle points (Figure 7). A low-lying early encounter complex (EC) between nucleophile and radical cation precedes the much later actual barrier to C−O bond formation. This profile was generated by carrying out ∼40 partial geometry optimizations (UHF/6-31G*) with fixed C_2−O distances in 5−10 pm increments. The results for nucleophilic attack anti and syn to the cyclopropane function yield very similar curves. The two encounter complexes have a negligible energy difference (EC_{syn} lies 0.07 kcal/mol higher) and long C_2−O interaction distances (∼290 pm for EC_{anti}, ∼330 pm for EC_{syn}). The transition states (TS's), lie 8−9 kcal/mol above the encounter complexes (Figures 8 and 9); approach of methanol anti to the cyclopropane ring is favored by ∼0.9 kcal/mol over the syn approach. The small energy difference is most likely the result of steric repulsion between methanol and the cyclopropane function (Figure 10). The C_2−O distances of both transition states are almost identical (181.5 pm for TS_{anti} vs 181.4 pm for TS_{syn}), indicating similarly rehybridized C_2 atoms. The energy difference between the transition states for capture of the bridged radical cation, $\mathbf{3}^{\bullet+}$, relative to the model system, $\mathbf{1}^{\bullet+}$, is very likely reduced, because the difference in steric congestion anti and syn to the cyclopropane ring should be attenuated by the presence of the bridge (Figure 11). This conclusion is borne out by the comparable yields of products **4** and **5**. Interestingly,

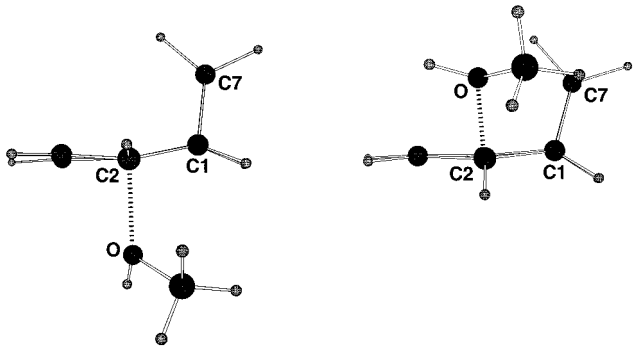

Figure 10. "Side" view of the transition states; syn (left) or anti (right) to the cyclopropane ring.

(43) (a) Gassman, P. G.; Olson, K. D. *Tetrahedron Lett.* **1983**, *1*, 19. (b) Weng, H.; Roth, H. D. *J. Org. Chem.* **1995**, *60*, 4136−4145.

(44) (a) Shaik, S. S.; Dinnocenzo, J. P. *J. Org. Chem.* **1990**, *55*, 3434. (b) Shaik, S. S.; Reddy, A. C.; Ioffe, A.; Dinnocenzo, J. P.; Danovich, D.; Cho, J. K. *J. Am. Chem. Soc.* **1995**, *117*, 3205−3222.

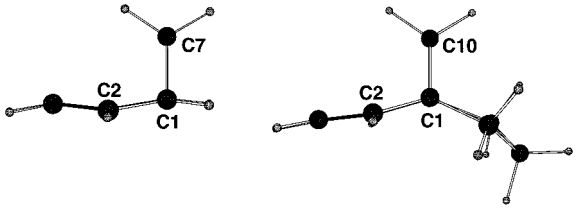

Figure 11. "Side" views of norcaradiene radical cation, $\mathbf{1}^{\bullet+}$, and the bridged analogue, $\mathbf{3}^{\bullet+}$.

attack at the cyclopropane carbons fails to lead to a transition state; a methanol molecule placed near $\mathbf{1}^{\bullet+}$, within 200−250 pm of $C_{1,6}$ or C_7, is repelled.

The rather short C−O bond distances between nucleophile and substrate radical cation are characteristic for "late" transition states, in contrast to the "early" transition states previously suggested for the capture of phenylcyclopropane radical cations.[35a] Shaik and co-workers found a C−O interaction distance of 207 pm for the backside attack of water on cyclopropane radical cation (HF/6-31G*).[44b]

The different interaction distances obtained by these calculations for the transition states may indicate that the nucleophilic capture by cyclopropane (S_N2-like, "substitution") and alkene radical cations (S_N1-like, "addition") have different requirements. Similar reaction profiles and transition states were also obtained when the nucleophilic capture of *cis*-butadiene or vinylcyclopropane radical cations were modeled by *ab initio* methods.[45] We note that there is no linear correlation between interaction distance and barrier to bond formation. Rather, the molecular orbital effects delineated earlier in this paper govern the approach of the nucleophile and the favored free-radical "product(s)". The short nucleophile−substrate interaction distances computed for attack of methanol on $\mathbf{1}^{\bullet+}$ warrant further exploration. Nevertheless, the calculations fully support the key features of the experimental results: the regiochemistry of attack is confirmed by facile approach of the nucleophile to C_2; the attack on C_7 (C_{10}) is unfavorable, despite the involvement of the cyclopropane ring in delocalizing spin and charge; and the limited stereochemical preference is borne out by the marginal energy difference between the transition states for attack either syn or anti to the cyclopropane ring.

The emerging principles governing the nucleophilic attack on bi- or trifunctional radical cationic systems are being tested as well as further elaborated in additional substrates using experimental and theoretical approaches.

Acknowledgment. Financial support of this work by the National Science Foundation through grants NSF CHE-9414271 and CHE-9714850 and an equipment grant NSF CHE-9107839 is gratefully acknowledged. The work of F.B. was supported by an NSF undergraduate equipment grant, NSF USE-9250530, for the purchase of a 200 MHz FT NMR spectrometer. A generous allocation of supercomputer time from NCSA (CHE980003N) at Urbana−Champaign, Illinois, is also gratefully acknowledged.

Supporting Information Available: NMR spectral assignments and MS data for products **4** and **5** (5 pages, print/PDF). See any current masthead page for ordering information and Web access instructions.

JA9732035

(45) Herbertz, T.; Roth, H. D. Unpublished results.